

Surface dielectric functions of a free-electron gas

J. E. Miraglia and M. S. Gravielle

Instituto de Astronomía y Física del Espacio, Consejo Nacional de Investigaciones Científicas y Técnicas, Departamento de Física, Facultad de Ciencias Exactas y Naturales, Universidad de Buenos Aires, Casilla de Correo 67, Sucursal 28, 1428 Buenos Aires, Argentina

(Received 5 March 2002; published 23 September 2002)

We investigate the surface dielectric response of a free-electron gas to a projectile moving parallel to the surface. Three theoretical models are examined, viz., the specular reflection and the parallel dispersion models, and a here-proposed axial model. The mean-free path, the stopping, the straggling, and the self-induced potential at the projectile position, are calculated in terms of the distance of the projectile to the surface. Differences at level of energy-loss distribution are found. We conclude that the axial model is reliable, has a simple closed form and permits us to estimate the binary contribution.

DOI: 10.1103/PhysRevA.66.032901

PACS number(s): 34.50.Bw, 73.20.Mf

I. INTRODUCTION

As a heavy projectile collides with a metal surface, it interacts with the valence electrons and the inner shells of the target atoms. The most relevant quantity to determine the moment (\mathbf{q}) and energy (ω) ceded by the projectile to the valence electrons is the screened projectile potential. Inside metal solids, one can consider, when possible, the valence electrons as a free-electron gas. In the bulk, the geometry of the interaction has an axial symmetry with the rotation axis along \mathbf{v} , where \mathbf{v} is the ion velocity. The Fourier transform of the *bulk* screened potential reads $W(q, \omega) = V(q)/\varepsilon(q, \omega)$, where $V(q)$ is the Fourier transform of the Coulomb potential, $q = |\mathbf{q}|$, $\omega = \mathbf{q} \cdot \mathbf{v}$, and $\varepsilon(q, \omega)$ is the Lindhard dielectric-response function [1].

The problem we face in this work consists of extending the dielectric formalism to deal with projectiles moving parallel to the surface, instead of moving well inside the bulk [2,3]. In general, one expects that the Fourier transform of the *surface* screened interaction $W(\mathbf{R}_0, \mathbf{q})$ to depend on \mathbf{R}_0 , the position of the projectile with respect to the surface, and $\mathbf{q} = (q_x, q_y, q_z)$, where $q_x = \omega/v$, q_z is the momentum transfer perpendicular to the surface, and q_y is the projection parallel to the surface and perpendicular to \mathbf{v} .

In similar fashion to the bulk, we can write $W(\mathbf{R}_0, \mathbf{q}) = V(\mathbf{R}_0, \mathbf{q})/\mathcal{E}^{(3)}(\mathbf{R}_0, \mathbf{q})$, where $\mathcal{E}^{(3)}(\mathbf{R}_0, \mathbf{q})$ is the here-called three-dimensional screening (dividing) factor. In principle, no symmetry is observed except that given by the planar surface. So we find convenient to write $\mathcal{E}^{(3)}(\mathbf{R}_0, \mathbf{q}) = \mathcal{E}^{(3)}(Z_0, q_{\parallel}, q_z, \omega)$ with $q_{\parallel} = (q_y^2 + \omega^2/v^2)^{1/2}$, and Z_0 is the distance to the jellium border ($Z_0 > 0$ vacuum, $Z_0 < 0$ solid). Deep inside the solid as $Z_0 \rightarrow -\infty$, we expect $\mathcal{E}^{(3)}(Z_0, \mathbf{q}) \rightarrow \varepsilon(q, \omega)$.

One of the more rigorous models to describe the surface dielectric function is the specular reflection model (SRM), which lets us obtain $\mathcal{E}_{SRM}^{(3)}(Z_0, q_{\parallel}, q_z, \omega)$ knowing of the bulk function $\varepsilon(q, \omega)$ [4–8]. To derive $\mathcal{E}_{SRM}^{(3)}$, it is assumed that the surface is a perfect plane situated at a precise position in which the “information” is reflected without interference. The solution of the so-posed problem leads us to *begrenzung* effect (the inhibition of bulk modes in favor of surface

modes in the surface region of the material). Although mathematically correct, to some extent the SRM simplifies real surfaces [3]. The position of the surface is not precise (although the widely accepted prescription is that the jellium border should be shifted half of the planar atom separation from the topmost atomic plane), and the full reflection at the surface implies an infinite barrier which is not realistic (metal barriers are of the order of the electron volts) [9,10]. Therefore, we could expect that in real surfaces *begrenzung* constrain may, if not be erased, at least be partially eroded.

Another model commonly employed is the parallel distortion model (PDM) [11,12]. It is derived employing the continuity of the potential and the displacement vector at the interface and considering only dispersion parallel to the surface. Also it can be derived from the SRM by neglecting the component of the moment perpendicular to the surface. This model has a simple closed form in terms of $\varepsilon(q_{\parallel}, \omega)$ but the cost, as we shall see, is that bulk limit is not satisfied but at high-impact energies [13].

In a recent article, García-Lekue and Pitarke [3] have reported self-consistent density-functional calculations of the density response function in surfaces, including exchange within the so-called adiabatic local-density approximation. The employed model considers the surface as a finite and smooth barrier, including quantum-mechanical interferences and the electronic selvage of the metal surface. Four major conclusions were drawn: (i) *begrenzung* inside the solid is diminished, (ii) surface-plasmon peak is considerably shifted towards smaller energies, (iii) bulk excitation is still present for trajectories outside the surface, and (iv) the influence of the exchange is not very relevant. Links with these calculations will be carried out along this work.

In the present paper we propose and explore a closed form for the dielectric function that we call axial model (AM). In essence, it keeps the simplicity of the PDM expression but recovers the axial symmetry proper to the ion moving well within the bulk. As we shall see, there are number of advantages of this model, such as a simple separation between binary and collective modes.

This paper presents comparative performances of these three models, SRM, PDM, and AM. Numerical results for the first three moments of the energy loss (i.e., mean-free

path, stopping and straggling) as well as the induced potential are reported and analyzed for protons colliding with aluminum surfaces for a wide range of impact energies (from 1 to 700 keV). In Sec. II, the basic formulae are presented, in Sec. III we display the numerical results, and Sec. IV contains the conclusion. Atomic units are used.

II. THEORY

The induced potential created by a punctual charge Z_P moving parallel to the surface to a distance Z_0 at the charge position, can be expressed in terms of the three-dimensional screening factor $\mathcal{E}^{(3)}$ as follows:

$$V^{ind}(Z_0) = \frac{Z_P}{2\pi^2} \int \frac{d\mathbf{q}}{q^2} \left[\frac{1}{\mathcal{E}^{(3)}(Z_0, \mathbf{q})} - 1 \right]. \quad (1)$$

Axial symmetry implies that $\mathcal{E}^{(3)}(Z_0, \mathbf{q}) = \mathcal{E}^{(3)}(Z_0, q, \omega)$ and so it is convenient to express $d\mathbf{q} = 2\pi/v dq d\omega$. For planar symmetry, we integrate Eq. (1) on q_z , to yield

$$V^{ind}(Z_0) = \frac{Z_P}{2\pi} \int \frac{dq_{\parallel}}{q_{\parallel}} \left[\frac{1}{\mathcal{E}^{(2)}(Z_0, q_{\parallel}, \omega)} - 1 \right], \quad (2)$$

where $\mathcal{E}^{(2)}$ is the bidimensional screening factor. It is here convenient to express $d\mathbf{q}_{\parallel} = 2/v F(q_{\parallel}, \omega) dq_{\parallel} d\omega$, where

$$F(q_{\parallel}, \omega) = \frac{q_{\parallel}}{\sqrt{q_{\parallel}^2 - (\omega/v)^2}}. \quad (3)$$

We will concentrate on three linear models.

(i) The specular reflection model (SRM). The inverse of the bidimensional screening factor used in Eq. (2) is found to be

$$\begin{aligned} \frac{1}{\mathcal{E}_{SRM}^{(2)}(Z_0, q_{\parallel}, \omega)} &= \left[1 + \frac{1 - \mathcal{E}_S(0, q_{\parallel}, \omega)}{1 + \mathcal{E}_S(0, q_{\parallel}, \omega)} E(q_{\parallel}) \right] \Theta(Z_0) \\ &+ \left[1 + \frac{\mathcal{E}_S(0, q_{\parallel}, \omega)}{\mathcal{E}_S(2Z_0, q_{\parallel}, \omega)} \right. \\ &\left. - \left(\frac{\mathcal{E}_S(0, q_{\parallel}, \omega)}{\mathcal{E}_S(Z_0, q_{\parallel}, \omega)} \right)^2 \frac{2}{1 + \mathcal{E}_S(0, q_{\parallel}, \omega)} \right] \\ &\times \frac{1}{\mathcal{E}_S(0, q_{\parallel}, \omega)} \Theta(-Z_0), \end{aligned} \quad (4)$$

$E(Q) = \exp(-2Q|Z_0|)$, Θ is the Heaviside function and \mathcal{E}_S is given by

$$\frac{1}{\mathcal{E}_S(Z, q_{\parallel}, \omega)} = \frac{q_{\parallel}}{\pi} \int_{-\infty}^{\infty} \frac{dk_z}{q_{\parallel}^2 + k_z^2} \frac{\exp(ik_z Z)}{\varepsilon[(q_{\parallel}^2 + k_z^2)^{1/2}, \omega]}. \quad (5)$$

(ii) The parallel dispersion model (PDM). This model can be derived from $\mathcal{E}_{SRM}^{(2)}$ by neglecting in the integral of Eq. (5) the dependence on k_z of ε , namely, $\varepsilon[(q_{\parallel}^2 + k_z^2)^{1/2}, \omega]$

$\approx \varepsilon[q_{\parallel}, \omega]$, or equivalently $\mathcal{E}_S^{-1}(Z, q_{\parallel}, \omega) = \exp(-q_{\parallel}|Z|)/\varepsilon(q_{\parallel}, \omega)$. By replacing this expression in Eq. (4), it yields

$$\begin{aligned} \frac{1}{\mathcal{E}_{PDM}^{(2)}(Z_0, q_{\parallel}, \omega)} &= [1 + R(q_{\parallel}, \omega) E(q_{\parallel})] \Theta(Z_0) \\ &+ [1 - R(q_{\parallel}, \omega) E(q_{\parallel})] \\ &\times \frac{1}{\varepsilon(q_{\parallel}, \omega)} \Theta(-Z_0), \end{aligned} \quad (6)$$

with

$$R(Q, \omega) = \frac{1 - \varepsilon(Q, \omega)}{1 + \varepsilon(Q, \omega)}. \quad (7)$$

(iii) The axial model (AM), that we introduce here, permits to absorb momentum perpendicular to the surface and its expression to be used in Eq. (1) is found to be

$$\begin{aligned} \frac{1}{\mathcal{E}_{AM}^{(3)}(Z_0, q, \omega)} &= [1 + R(q) E(q'_{\parallel})] \Theta(Z_0) \\ &+ [1 - R(q) E(q'_{\parallel})] \\ &\times \frac{1}{\varepsilon(q, \omega)} \Theta(-Z_0). \end{aligned} \quad (8)$$

with

$$q'_{\parallel} = \sqrt{\frac{1}{2} \left(q^2 + \frac{\omega^2}{v^2} \right)}. \quad (9)$$

We have derived this expression from the SRM following two considerations. (i) The full screening factor $\mathcal{E}_{SRM}^{(3)}(Z_0, \mathbf{q})$ has been expressed in terms of an Fourier integral on k_z as the one given by Eq. (5). Next we evaluate the integrand at $k_z = q_z$ to satisfy the bulk limit. Thus $\varepsilon(q, \omega)$ is extracted from the integrand of Eq. (5) instead of $\varepsilon(q_{\parallel}, \omega)$ corresponding to the peaking approximation ($k_z = 0$) used in the PDM. (ii) The argument q_{\parallel} of E has been transformed to q'_{\parallel} imposing again the axial approximation. If $q^2 = q_z^2 + q_y^2 + (\omega/v)^2$, the axial symmetry imposes $q_y = q_z$, then $q_y^2 = [q^2 - (\omega/v)^2]/2$, and so $q_{\parallel}^2 = (q^2 + \omega^2/v^2)/2 = q'^2_{\parallel}$ as given by Eq. (9).

The physics underlying these points can be observed by inspecting the induced potentials. In the PDM, the interaction potential is screened by $\mathcal{E}_{PDM}^{(2)}(Z_0, q_{\parallel}, \omega)$ implying a cutoff just in the plane parallel to the surface but remaining essentially Coulombian in the z direction. On the contrary in the AM, the presence of $R(q, \omega)$ instead of $R(q_{\parallel}, \omega)$ introduces a cutoff in the z -direction similar to that in the plane parallel to the surface. In this way the planar symmetry of the PDM becomes an axial one in the AM. In other words, the PDM as well as the AM are rooted in the SRM, but while the

PDM is derived by considering planar symmetry (by imposing $k_z=0$), the AM is derived by considering axial symmetry ($q_y=q_z=k_z$).

A. The energy loss moments and the induced potential

The moments of the energy loss can be written as

$$P^{(n)}(Z_0) = \int_0^\infty d\omega \frac{dP(Z_0)}{d\omega} \omega^n. \quad (10)$$

The probability $P^{(0)}=P=\Lambda^{-1}$ (or the inverse of the mean-free path) corresponds to $n=0$, the stopping $P^{(1)}=S$ corresponds to $n=1$, and the second moment is the straggling $P^{(2)}=\Omega^2$. Since the calculation of the energy-loss spectrum $dP(Z_0)/d\omega$ requires the integral on the momentum transfer $\int d\mathbf{q}$, it is convenient to express it in terms of the variables suitable to the symmetry under study. For the SRM and PDM, where planar symmetry is observed, it is found from Eqs. (2)

$$\frac{dP_X(Z_0)}{d\omega} = S_0 \int_{\omega/v}^\infty \frac{dq_{\parallel}}{q_{\parallel}} F(q_{\parallel}, \omega) \text{Im} \left[\frac{1}{\mathcal{E}_X^{(2)}(Z_0, q_{\parallel}, \omega)} \right], \quad (11)$$

X =SRM or PDM and $S_0 = -2Z_p^2/(\pi v^2)$.

For the AM, where axial symmetry is satisfied, the natural set of variables in common with any bulk dielectric function is recovered, and from Eq. (1),

$$\frac{dP_{AM}(Z_0)}{d\omega} = S_0 \int_{\omega/v}^\infty \frac{dq}{q} \text{Im} \left[\frac{1}{\mathcal{E}_{AM}^{(3)}(Z_0, q, \omega)} \right]. \quad (12)$$

In this way the AM shrinks to a simple screening function with the same symmetry to that of the bulk but depending parametrically on Z_0 .

The energy-loss moments depend on the imaginary part of the inverse of the screening factor, while the potential created by the projectile depends on the real part. From Eqs. (1) and (2), the induced potential at the projectile position $V^{ind}(Z_0)$ can be reduced to an expression similar to Eqs. (10)–(12) ($n=0$), with the real part minus one instead of the imaginary one and $V_0=2Z_p/(\pi v)$ instead of S_0 . The so-called image potential (self-interaction), which is the relevant quantity to calculate the ion trajectory, is one-half of the induced potential [4]. Detail examinations of the surface and bulk induced potentials are given in Appendix A of Ref. [12]

B. Bulk limits

We prove here that the proper bulk limit (as $Z_0 \rightarrow -\infty$) is satisfied by the AM and SRM but not by the PDM. In the first case, it is obvious from Eq. (8) that $\mathcal{E}_{AM}^{(3)}(Z_0, q, \omega) \rightarrow \varepsilon(q, \omega)$, and therefore the bulk result is restored. Similar limit holds for the SRM as explained below. Thus by $\mathcal{E}_{SRM}^{(2)}(Z_0, q_{\parallel}, \omega) \rightarrow \mathcal{E}_S(0, q_{\parallel}, \omega)$, replacing this limit in Eq. (2) and writing $k_z \equiv q_z$, the integral $\int d\mathbf{q}$ can be restored, so the axial symmetry is recovered and the bulk expression in terms

of $\varepsilon(q, \omega)$ is reproduced. The SRM then has the virtue of describing the bulk limit, changing from planar symmetry outside the solid to axial symmetry deep inside. We consider the SRM as a good reference to compared with.

For the PDM, as $Z_0 \rightarrow -\infty$, $\mathcal{E}_{PDM}^{(2)}(Z_0, q_{\parallel}, \omega) \rightarrow \varepsilon(q_{\parallel}, \omega)$ thus the energy-loss probability tends to

$$\frac{dP_{PDM}}{d\omega} \rightarrow S_0 \int_{\omega/v}^\infty \frac{dq_{\parallel}}{q_{\parallel}} F(q_{\parallel}, \omega) \text{Im} \left[\frac{1}{\varepsilon(q_{\parallel}, \omega)} \right]. \quad (13)$$

By writing $q_{\parallel} \equiv q$ the integrand remains the same as the bulk limit [Eq. (13)] except for the multiplicative factor $F(q_{\parallel}, \omega)$. This factor is responsible for the failure (overestimation in all the cases) of the PDM at intermediate and small velocities. In the limit as $v \rightarrow \infty$, $F(q_{\parallel}, \omega) \rightarrow 1$, and only in this case the PDM tends to the proper value.

III. NUMERICAL RESULTS.

Three numerical integrations are required to obtain the energy-loss moments for the SRM (on k_z , q_{\parallel} , and ω), and just two for the PDM (on q_{\parallel} and ω) and AM (on q and ω). Deep inside the solid, care should be paid to integrate on k_z in Eq. (5) due to the oscillatory pattern with Z_0 . Mermin Lindhard dielectric-response function was used to represent the free-electron gas [1,14]. For aluminum target, the following parameters were considered: volume (bulk)-plasmon energy $\omega_v=0.566$ and the life time $\gamma=0.0375$ [15].

Stopping results are presented in Fig. 1 for protons colliding with aluminum surfaces as a function of the distance to the jellium border (Z_0) for four impact energies ranging from 1 to 700 keV. Regardless of the impact velocity, the agreement between the AM with the SRM is very good. As mentioned before, in all the cases, the PDM overestimates the SRM results, tending to the Lindhard values inside the solid only in the high-velocity limit. The same performance was found for the probability (Fig. 2), straggling (Fig. 3) and induced potential at the projectile position (Fig. 4). Only in the case of very high-impact velocity ($v \rightarrow \infty$) and long distance to the surface ($Z_0 \rightarrow +\infty$, where the probability is negligible), the PDM seems to approach the SRM better than the AM. From the examination of Fig. 1, and as far as the free-electron gas role is concerned, we *cannot* say that $S(Z_0)$ decays as an exponential as it is widely accepted in the experimental domain [16,17]. Although, at high impact energies, the classical expression of Echenique and Pendry [18] provides a very good estimate for $Z_0 \rightarrow +\infty$.

At long distances, the induced potential at the projectile position behaves as Coulombic due to the interaction with its image charge [15]. In Fig. 4, we plot also the Coulomb potential, which satisfies the value given by the SRM at $Z_0=5$, with dash-dotted lines. Note that at 700-keV proton impact, the induced potential does not behave as Coulombic yet around $Z_0=5$.

As far as the energy-loss moments are concerned, the AM is a good candidate to replace the SRM when the numerical calculation requires computational economy [12]. We have reached energies as low as 1 keV to show that the AM is still

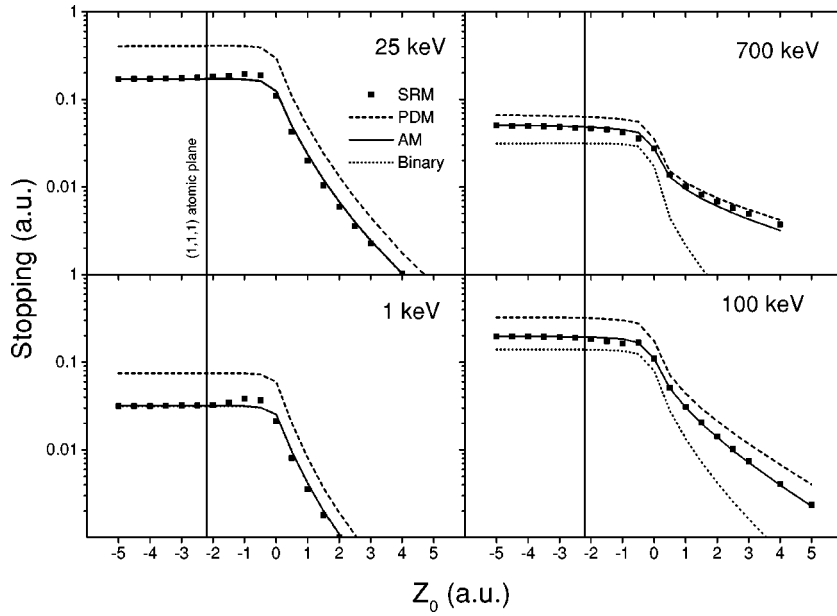


FIG. 1. Stopping cross sections for protons on aluminium as a function of the distance of the projectile with respect to the jellium border Z_0 . Impact proton energies as indicated. Notation: Squared symbols, the SRM; dashed line PDM; solid line, AM; and dotted line binary contribution of the AM.

a good approximation to the SRM, even though the linear response function is out of range of validity.

The spectacular agreement between the SRM and the AM at level of integrated values does not mean that the energy-loss spectra also agree with each other. To inspect in detail the differences, in Fig. 5 we plot the spectra for 700 keV protons on aluminum (case studied theoretically by Juaristi *et al.* [4], and experimentally by Winter *et al.* [17]). Three values for the penetration are presented; outside the solid $Z_0=2$; at the jellium border $Z_0=0$, and well inside $Z_0=-5$. Certainly for $Z_0 \geq 0$ the three models agree each other and no appreciable differences are found. All of them display one peak at the surface-plasmon frequency $\omega_s = \omega_v / \sqrt{2} = 0.4$. The situation is different well inside the solid. For $Z_0 = -5$, the SRM predicts the major contribution coming from surface-plasmon excitations at ω_s due to begrenzung effect. The AM and PDM predict two peaks instead: at the

surface (ω_s) as well as at the volume-plasmon (ω_v) frequencies, with larger contribution coming from the latter. As we penetrate deeper, both SRM and AM tend to the Lindhard results (just one peak at ω_v for, say, $Z_0 < -10$).

By comparing the present findings with the results of Ref. [3] one feature is missing in the present calculation; no trace of bulk plasmon for $Z_0 \geq 0$ is found. But in accordance with Ref. [3], an appreciable shift of the surface-plasmon peak towards smaller energies is found. For 100-keV incident protons at $Z_0 = +3.38$, the AM peak is shifted 0.08 a.u. (2.2 eV) from that of the SRM while the shift between the RPA and the SRM calculations in Ref. [3] is 0.12 a.u. (3.2 eV). It would mean that axial symmetry is a step in the direction of including finite barrier. Also, we find that begrenzung effect is diminished, i.e., the bulk-plasmon peak becomes rapidly relevant as we penetrate the solid when compared with the SRM.

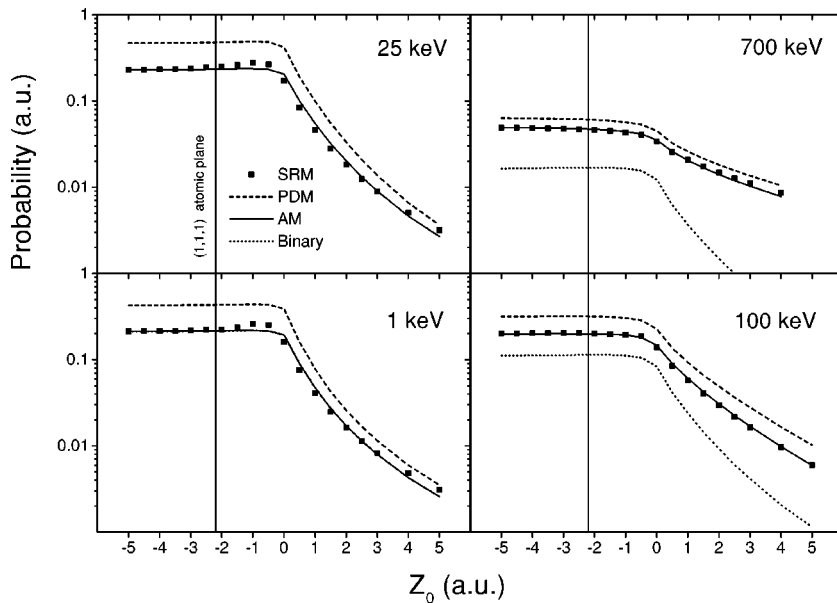


FIG. 2. Similar to Fig. 1 for the probability (or inverse of the mean-free path).

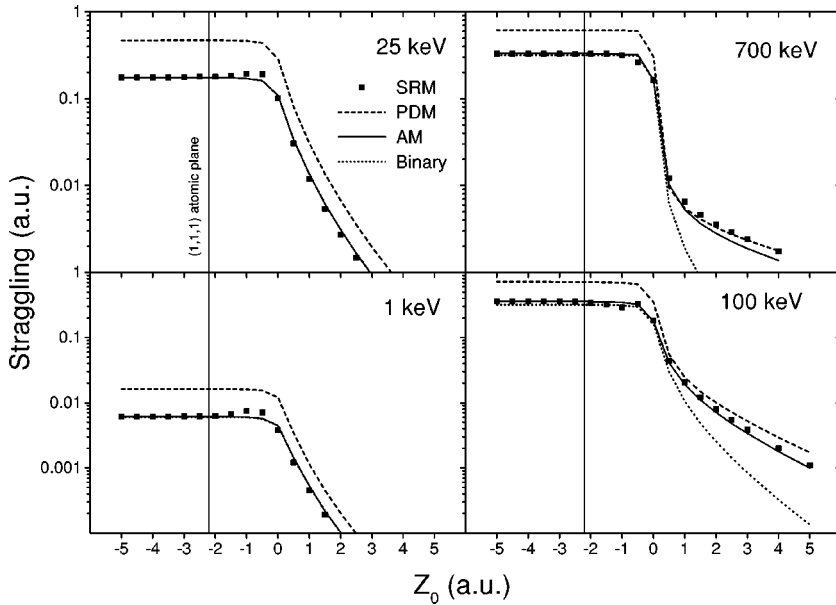


FIG. 3. Similar to Fig. 1 for the straggling.

These results could be important to understand a series of recent experiments which have found that grazing reflected ions produce electrons escaping from the surface with energies near the bulk-plasmon values [19]. The given explanation is based on the assumption that electrons produced by the impinging projectile excite the bulk (instead of surface) plasmon, and decay follows transferring its energy to a free electron. Although the AM favors volume plasmons by comparing with surface ones, still the electrons should penetrate very deep inside, say $Z_0 < -10$, to fully excite the volume mode alone as the SRM. Perhaps the excitation of the volume plasmon found in the experiments [19] may be an indication of the deterioration of the strict begrenzung constrain of the SRM.

Binary contribution

Besides simplicity, we find that the AM has another important advantage: due to the axial symmetry, it is possible to

estimate the binary contribution. It can be achieved by multiplying the integrand by the well-known factor [21]

$$U(q, \omega) = \Theta[q^2 k_F^2 - (\omega - q^2/2)^2]. \quad (14)$$

This factor reduces the integration to the binary band, conserving energy and momentum in a collision with a single electron. Binary AM results are presented in Figs. 1, 2, 3, and 5 with dotted lines. The limits are correct. At low-impact velocities, $v < v_0 = 1.2$ for aluminum, collective oscillations are not present, and so all the contribution comes from binary encounters alone [20]. At larger velocities and well inside the solid, the binary stopping equals that of the collective mode, as expected due to the equipartition rule [21]. Outside the solid, binary contribution vanishes, leaving the excitation of surface plasmon as the only mechanism of stopping, as predicted by Lucas [22] and Kawai [23]. We can also determine the importance of the binary contribution in-

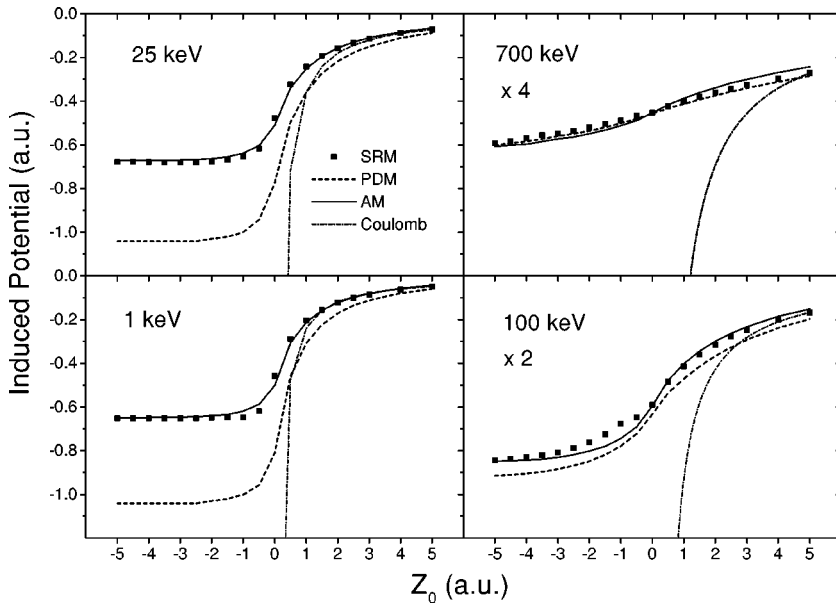


FIG. 4. Similar to Fig. 1 for the induced potential at the projectile position.

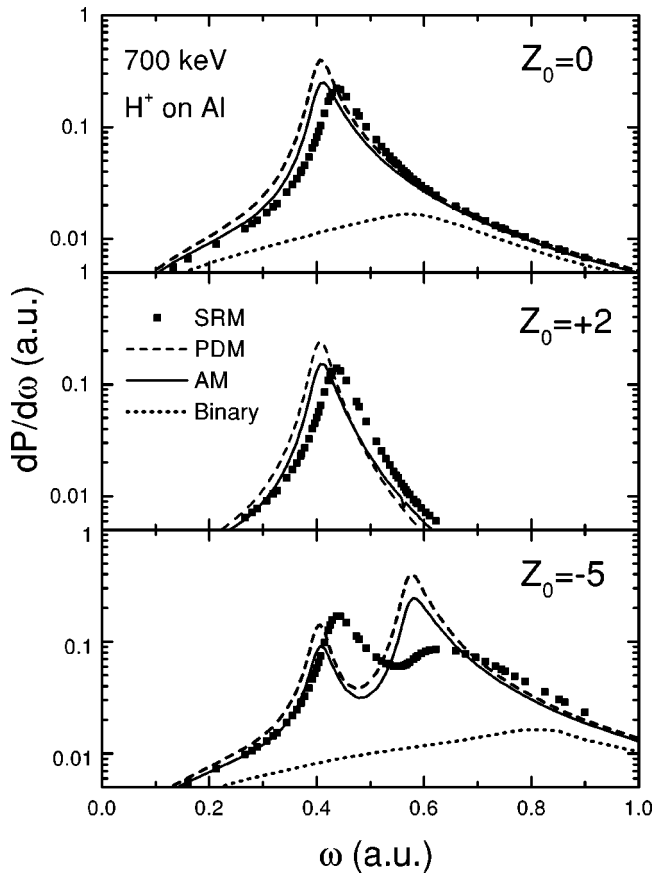


FIG. 5. Energy-loss distributions for 700 keV protons on Al. Notation similar to Fig. 1.

side the solid with increasing moment n . For the probability ($n=0$), binary contribution for $v > v_0$ is just a small fraction of the total (in this case the mean-free path is determined mainly between two successive plasmon excitations). Binary contribution to the probability is an important quantity since it represents the integrated production of primary electrons. For the stopping ($n=1$), the binary contribution represents the half, while for the straggling ($n=2$) it accounts for al-

most the total. Except far outside the solid where the surface collective mode is still the most relevant, as found experimentally by Kimura *et al.* [24].

This simple separation of the binary contribution from the total can be done *only* in the AM and not in the SRM (not in the PDM). To extract binary information from the SRM and PDM following the same criteria, a tedious algebra and an additional numerical integration are needed. More specifically, one should start over from the full expression of $\mathcal{E}_{SRM}^{(3)}(Z_0, q_{\parallel}, q_z, \omega)$, multiply by $U(q, \omega) = U((q_{\parallel}^2 + q_z^2)^{1/2}, \omega)$, and integrate on the variables q_{\parallel} and q_z to obtain the energy spectra. The results were found to be not reliable (very unstable and oscillatory) and we consider them not worth publishing.

By subtracting the binary contribution from the total value, we can determine the collective excitation. Further, as an unexpected by-product, let us estimate the contribution from the volume as well as the surface collective contribution by simply separating the enhancements centered on ω_v and ω_s peaks, respectively.

IV. CONCLUSIONS

We have studied in detail the first three moments of the energy loss, i.e., probability, stopping and straggling, with the three models, SRM, PDM, and AM, for a wide range of impact energies, from very low (1 keV) to high energies (700 keV). We have observed that the PDM does not tend to the proper bulk limit inside the solid. Instead the AM here-proposed behaves very well, and its properties are summarized as: (i) it has a very simple closed form, (ii) there is no appreciable difference with the SRM at the level of the integrated values of the first three moments and the induced potential, (iii) the binary contribution can be easily extracted, (iv) by subtracting, collective contribution can be estimated, and the surface and volume modes can be separated, (v) surface-plasmon peak is considerably shifted towards smaller energies, and (vi) begrenzung effects are diminished. Experiments are welcome to determine the quantitative importance of begrenzung. A minor setback has been found; for $v \rightarrow \infty$ and $Z_0 \rightarrow \infty$ (where the probability is negligible), the AM lightly underestimates the SRM prediction

- [1] J. Lindhard, Mat. Fys. Medd. K. Dan. Vidensk. Selsk. **28**, 8 (1954).
- [2] J. L. Gervasoni, Doctoral thesis, Universidad Nacional de Cuyo, 1992.
- [3] A. García Iekue and J. E. Pitarke, Phys. Rev. B **64**, 035423 (2001).
- [4] J. I. Juaristi, F. J. García de Abajo, and P. M. Echenique, Phys. Rev. B **53**, 13 839 (1996).
- [5] R. H. Ritchie and A. L. Marusak, Surf. Sci. **4**, 234 (1966).
- [6] R. Nuñez, P. M. Echenique, and R. H. Ritchie, J. Phys. C **13**, 4229 (1980).
- [7] F. Flores and García Moliner, J. Phys. C **12**, 907 (1979).
- [8] J. Heinrichs, Phys. Rev. B **8**, 1346 (1973).
- [9] E. V. Chulkov, V. M. Silkin, and P. M. Echenique, Surf. Sci. **437**, 330 (1999).
- [10] P. M. Echenique, J. M. Pitarke, E. V. Chulkov, and A. Rubio, Chem. Phys. **251**, 1 (2000).
- [11] J. Burgdörfer, *Progress in Atomic and Molecular Physics*, edited by C. D. Lin (World Scientific, Singapore, 1993).
- [12] C. O. Reinhold and J. Burgdörfer, Phys. Rev. A **1**, 450 (1997).
- [13] M. S. Gravielle, D. G. Arbó, and J. E. Miraglia, Nucl. Instrum. Methods Phys. Res. B **182**, 29 (2001).
- [14] D. Mermin, Phys. Rev. B **1**, 2362 (1970).
- [15] N. Arista, Phys. Rev. A **49**, 1885 (1994).
- [16] K. Kimura, H. Hasegawa, and M. Mannami, Phys. Rev. B **36**, 7 (1986).
- [17] H. Winter, M. Wilke, and M. Bergomaz, Nucl. Instrum. Methods Phys. Res. B **125**, 124 (1997).
- [18] P. M. Echenique and J. B. Pendry, J. Phys. C **8**, 2935 (1975).
- [19] E. A. Sanchez, J. E. Gayone, M. L. Martiarena, O. Grizzi, and

- R. Baragiola, Phys. Rev. B **61**, 14 209 (2000).
- [20] M. Wilke, R. Zimny, and H. Winter, Nucl. Instrum. Methods Phys. Res. B **100**, 396 (1995).
- [21] D. Arbó and J. E. Miraglia, Phys. Rev. A **55**, 3518 (1998).
- [22] A. A. Lucas, Phys. Rev. B **20**, 4990 (1979).
- [23] R. Kawai, N. Itoh, and Y. H. Ohtsuki, Surf. Sci. **114**, 137 (1982).
- [24] K. Kimura, H. Kurada, M. Fritz, and M. Mannami, Nucl. Instrum. Methods Phys. Res. B **100**, 356 (1995).